Available online at www.sciencedirect.com
SCIENCE DIRECT
Journal of Asian Earth Sciences 23 (2004) 467–482
Journal of Asian Earth Sciences
www.elsevier.com/locate/jseaes

Geochemical and isotopic constraints on the petrogenesis of granitoids from the Dalat zone, southern Vietnam

Nguyen Thi Bich Thuy[a,b,*], Muharrem Satir[a], Wolfgang Siebel[a], Torsten Vennemann[a], Trinh Van Long[c]

[a]*Institute of Geosciences, Universität Tübingen, Wilhelmstr. 56, D-72074 Tübingen, Germany*
[b]*Research Institute of Geology and Mineral Resources, Thanh Xuan-Dong Da, Hanoi, Viet Nam*
[c]*Union of Geological Mapping of Southern Vietnam, 200 Ly Chinh Thang, Ho Chi Minh city, Viet Nam*

Received 4 June 2002; revised 3 January 2003; accepted 30 June 2003

Abstract

Late Mesozoic granitoids of the Dalat zone are of sub-alkaline affinity, belong to the high-K calc-alkaline series and display features typical of I-type granites. The Dinhquan suite consists of hornblende-biotite granodiorites, diorites, and minor granites emplaced at ~110 My. These rocks have relatively low initial $^{87}Sr/^{86}Sr$ ratios (0.7049–0.7061) and moderate $\varepsilon_{Nd(T)}$ values (−0.8 to −2.0). Chondrite-normalized REE patterns are fractionated and have small negative Eu anomalies (Eu/Eu* = 0.55–0.97). All these characteristics, combined with low $Al_2O_3/(FeO + MgO + TiO_2)$ and $(Na_2O + K_2O)/(FeO + MgO + TiO_2)$ ratios and high Mg# values, suggest an origin through dehydration melting of alkaline mafic lower crustal source rocks. The Cana suite contains biotite-bearing granites poor in hornblende. The rocks are 96–93 My old in age, having higher initial $^{87}Sr/^{86}Sr$ ratios (0.7060–0.7064) and nearly constant $\varepsilon_{Nd(T)}$ (−2.5 to −2.7) values. These characteristics, in conjunction with the chemical signatures and old T_{DM} model ages, indicate that crustal material played a very important role in their petrogenesis. The granites are further characterized by strong negative Eu anomalies (Eu/Eu* = 0.04–0.39) and Sr, suggesting melting with residual plagioclase and/or a high degree of fractional crystallization. The Deoca suite is made up of 92–88 My old pink porphyritic hornblende-biotite-bearing granodiorites, monzogranites and diorites. Initial isotopic compositions ($^{87}Sr/^{86}Sr$ = 0.7055–0.7069; $\varepsilon_{Nd(T)}$ = +0.9 to −3.3) and chemical features suggest derivation by dehydration melting of heterogeneous metagreywacke-type sources with additional input of mantle-derived material. Furthermore, the Deoca rocks have concave-upward REE patterns indicating that amphibole played a dominant and garnet an insignificant role during magma segregation.

Keywords: Southern Vietnam; Dalat zone; High-K granitoids; Petrogenesis

1. Introduction

The numerous granitoids and contemporary volcanic rocks in the Dalat zone, southern Vietnam, are interpreted as resulting from the subduction of Western-Pacific oceanic crust beneath the SE-Asian continent during the Cretaceous (Taylor and Hayes, 1983). The petrography and mineralogy of these rocks are well studied, but knowledge of the origin, time of emplacement as well as geochemistry is limited. Few studies on the generation of the granitoids are available and most of them are written in Vietnamese and are hardly accessible to the international community. The Dinhquan and Deoca granitoids were formerly classified as I-type granites, whereas the Cana granites were thought to be of S-type (e.g. Hung, 1999). However, this classification must be regarded with care because key data to identifying the type and origin of a granite, including geochemical and isotopic data, were not available. This paper focuses on the origin of the granitoids, using detailed geochemical and Nd-,Sr-, and O-isotopic analysis to further constraint their petrogenesis. The tectonic setting of these rocks is also discussed.

Abbreviations: VAG, volcanic-arc granitoids; syn-COLG, syn-collisional granitoids; WPG, within plate granitoids; ORG, ocean-ridge granitoids.

* Corresponding author. Tel.: +49-7071-2972601; fax: +49-7071-295713.
E-mail address: bichthuyde@yahoo.de (N.T.B. Thuy).

1367-9120/$ - see front matter
doi:10.1016/j.jseaes.2003.06.001

2. Geological setting

The Dalat zone (Fig. 1) and its counterpart, the Kontum massif, belong to the Indochina Block that consists of fragments of Gondwana and formed the Southeastern Asian continent during the Precambrian, Palaeozoic, and Mesozoic (e.g. Şengör et al., 1988; Metcalfe, 1988, 1996). The basement of the Dalat zone is not exposed. However, seismic data suggest that it is composed of mafic granulites and gneisses (Khoan and Que, 1984). Such rocks occur in the Kontum massif and K–Ar and Rb–Sr geochronology indicate Late Paleoproterozoic (1.8–1.7 Ga; Hai, 1986) and early Mesoproterozoic (1.6–1.4 Ga; Thi, 1985) ages, respectively. Mesozoic plutonic and contemporary volcanic rocks are widespread in the eastern part of the Dalat zone and are interpreted as subduction-related products (Taylor and Hayes, 1983). During the Neogene-Quaternary, basalts associated with pull-apart, extensional rifts were formed following the collision between Eurasia and the Indian plates (Barr and MacDonald, 1981).

On the basis of petrographical and mineralogical studies, the Dalat granitoids were subdivided into three suites: (1) the Dinhquan suite (Trung and Bao, 1980); (2) the Cana suite (Thang and Duyen, 1988) and (3) the Deoca suite (Trung and Bao, 1980). Rocks of the Dinhquan suite occur as a northeast trending belt south of the Kontum massif. The rocks are medium-grained hornblende-biotite diorites, granodiorites and rare granites. The major rock-forming

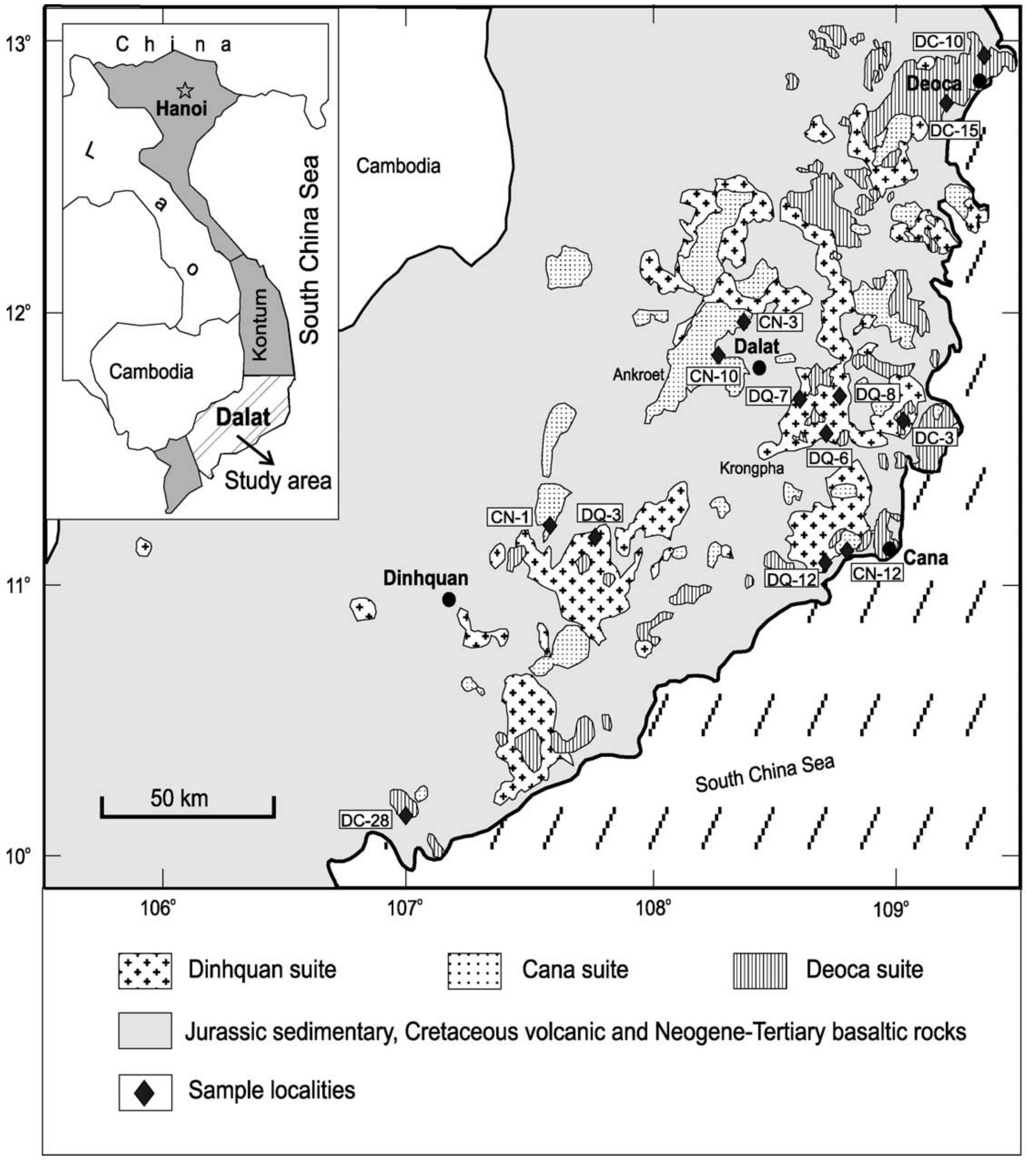

Fig. 1. Simplified geological map showing the distribution of the intrusive magmatic rocks in the Dalat zone (Tien et al., 1991).

mineral assemblage of the suite is plagioclase (oligioclase—andesine), K-feldspar (orthoclase—microcline), quartz, hornblende and biotite. Zircon, apatite and rare titanite are accessory phases. Plagioclase occurs as euhedral grains with twinning. Some grains are wellzoned. K-feldspar exhibits a microperthitic to perthitic texture, showing no twins and normally wrapped around euhedral plagioclase grains. Quartz is anhedral and displays undulatory extinction under X-polars. Hornblende is dark to palish green in color. Locally, hornblende underwent partial alteration to epidote and chlorite. Granodiorites contain small enclaves having dioritic composition.

Petrographically most of the Cana rocks are leucocratic biotite-bearing granites with scarce hornblende. These rocks are predominantly medium to coarse-grained displaying weakly porphyritic texture. In addition to quartz, K-feldspar, plagioclase, biotite, hornblende, and zircon, minor muscovite, tourmaline and cassiterite occur as post-magmatic products, observed at the top of small plutons or in greisenized granites. Quartz occurs as anhedral crystals with irregular distorted boundaries and normally occupies the interstices between feldspars. Plagioclase is generally euhedral, displaying fine twining or oscillatory zoning. K-feldspar occurs as anhedral to subhedral crystals. Biotite occurs as the minute flakes, scattered throughout the rocks. Biotite is usually chloritized and contains zircon inclusions. The Deoca suite is made up of medium-to coarse-grained granodioritic, monzogranitic and granitic rocks, forming a belt along the coast. The rocks are commonly pink, owing to abundant brick red K-feldspar, but cream-white K-feldspar is also present. The rocks exhibit porphyritic texture with K-feldspar phenocrysts. Plagioclase is normally zoned and the core is sericitized to varying degrees. Mafic minerals are hornblende and biotite. Titanite and zircon are commonly accessory minerals.

Rocks of the three suites intruded and metamorphosed the Jurassic Bandon Formation. As can be seen in the field, the Cana and Deoca granitoids clearly crosscut the Dinhquan granitoids, but contact relationships between the Cana and Deoca granitoids have not been observed. Zircon separated from rocks of all three suites were dated by the conventional U–Pb method and yielded concordant ages of $\sim 110 \pm 1$ My for the Dinhquan, 96–93 My for the Cana and 92–88 My for the Deoca suites (Thuy Nguyen et al., 2000).

3. Analytical methods

72 samples of 5–7 kg were crushed in a jaw crusher and powdered in an agate mill to avoid contamination. Major and trace element abundances were determined by wavelength X-ray fluorescence (XRF) spectrometry at the University of Tübingen using standard techniques. Loss on ignition (LOI) was calculated after heating the sample powder to 1000 °C for 1 h. Major and trace element analyses were performed on fused glass discs, which were made from whole-rock powder mixed with $Li_2B_2O_7$ (1.5:7.5) and fused at 1150 °C. Total iron concentration is expressed as Fe_2O_3. Analytical uncertainties range from ±1% to 8% and 5% to 13% for major and trace elements, respectively, depending on the concentration level.

The trace elements (Cs, Th, U, Ta, Hf, Sc and Pb) and the REE were determined by inductively coupled plasma-mass spectrometry (ICP-MS) at the Memorial University of St. John's Newfoundland, using the sodium peroxide (Na_2O_2) sinter technique, which ensures complete digestion of resistant REE-bearing accessory phases (e.g. zircon, allanite). For full details of the procedure, see Longerich et al. (1990). The precision and accuracy of the data have been reported by Dostal et al. (1986, 1994)).

For determination of Sr and Nd isotopic ratios, approximately 50 mg of whole-rock powdered samples were used. The samples were decomposed in a mixture of HF-$HClO_4$ in Teflon beakers in steel jacket bombs at 180 °C for six days to ensure the decomposition of refractory phases. Sr and Nd were separated by conventional ion exchange techniques and their isotopic compositions were measured on a single W filament and double Re filament configuration, respectively. A detailed description of the analytical procedures is outlined in Hegner et al. (1995). Isotopic compositions were measured on a Finnigan-MAT 262 multicollector mass spectrometer at the University of Tübingen using a static mode for both Sr and Nd. The isotopic ratios were corrected for mass fractionation by normalizing to $^{86}Sr/^{88}Sr = 0.1194$ and $^{146}Nd/^{144}Nd = 0.7219$. Total procedure blanks are <200 pg for Sr and <50 pg for Nd. During the course of this study, four analyses of standard NBS 987 yielded a mean value of $^{87}Sr/^{86}Sr = 0.710257 \pm 10$ (2σ). Measurements of the Ames Nd standard yielded a mean value of $^{143}Nd/^{144}Nd = 0.512129 \pm 10$ (2σ, $n = 5$). $^{87}Rb/^{86}Sr$ ratios for whole-rock samples were calculated based on the measured $^{87}Sr/^{86}Sr$ ratios and the Rb and Sr concentrations determined by XRF.

Oxygen isotope analyses were performed at the University of Tübingen. Oxygen was extracted from approximately 10 mg of dried whole-rock powder at 550 °C using BrF_5 as a reagent following the method of Clayton and Mayeda (1963). Quantitative oxygen yields were between 95 and 100%. The oxygen was converted to CO_2 using a graphite rod heated by a Pt-coil. CO_2 was analyzed for its $^{18}O/^{16}O$ ratios with a Finnigan MAT 252 gas source mass spectrometer. The isotopic ratios are reported in the δ-notation relative to Vienna standard mean ocean water (V-SMOW). All analyses have been duplicated with an analytical precision of between ±0.1–0.2‰. The analyses of NBS-28 standard quartz were $+9.7 \pm 0.1$‰ ($2\sigma_m$). All data have been normalized to NBS-28 = +9.7‰.

Table 1
Major (wt%) and trace element (ppm) abundances of representative samples from the Dinhquan (DQ), Deoca (DC), and Cana (CN) suites

Sample rock type	DQ-3 GrD	DQ-6 GrD	DQ-7 Gr	DQ-8 GrD	DQ-12 GrD	DC-3 GrD	DC-10 Gr
SiO_2	58.01	63.82	70.01	67.32	68.20	68.21	76.32
TiO_2	1.02	0.61	0.22	0.50	0.31	0.40	0.12
Al_2O_3	17.34	15.13	15.06	14.81	15.14	15.42	12.71
Fe_2O_3	7.02	5.81	3.04	3.92	3.71	3.60	1.14
MnO	0.12	0.12	0.11	0.07	0.08	0.05	0.01
MgO	2.81	2.40	0.52	1.61	1.20	1.41	0.11
CaO	6.23	4.33	2.11	3.35	3.32	3.62	0.95
Na_2O	3.11	2.81	4.05	2.95	3.25	3.06	3.32
K_2O	2.61	3.52	3.84	4.34	3.42	3.64	4.83
P_2O_5	0.32	0.21	0.11	0.11	0.21	0.11	0.13
H_2O	0.52	0.70	0.41	0.52	0.50	1.13	0.21
Total	99.11	99.46	99.68	99.18	99.34	100.63	99.85
ASI	0.90	0.92	1.02	0.96	1.01	0.99	1.03
Co	0	0.02	0.50	0.01	0.42	0.11	0.41
Cr	87	71	91	157	112	5	21
Ni	51	31	32	28	35	2	25
Sr	474	285	246	233	404	306	79
Ba	465	393	553	295	543	401	118
Zr	183	160	209	160	124	129	99
Rb	97	153	146	210	109	113	304
Cs	7.33	10.15	8.12	8.10	4.14	2.05	4.80
Hf	4.76	3.42	4.90	4.51	3.51	3.54	3.61
Nb	8.0	5.3	5.6	7.1	6.2	11.1	12.2
Ta	0.83	0.71	0.80	0.92	0.76	1.51	0.53
Th	10.3	12.6	15.6	29.2	10.6	14.4	41.3
U	2.25	1.87	2.36	5.41	3.12	3.91	20.32
Y	25	27	28	26	16	20	21
Pb	12	16	25	14	20	22	31
Zn	71	65	50	44	64	56	15
La	24.3	25.9	32.3	28.2	22.4	21.8	21.1
Ce	50.7	53.1	60.5	55.4	41.4	42.6	38.9
Pr	6.01	6.16	6.84	6.13	4.50	4.71	3.76
Nd	23.6	23.3	24.8	22.1	16.3	17.0	11.6
Sm	5.04	4.92	4.91	4.62	3.21	3.42	1.90
Eu	1.50	0.91	0.90	0.81	0.80	0.80	0.22
Gd	4.42	4.33	4.08	3.86	2.53	2.96	1.51
Tb	0.65	0.62	0.63	0.63	0.42	0.51	0.23
Dy	3.91	4.10	3.82	3.45	2.24	2.84	1.60
Ho	0.83	0.95	0.85	0.70	0.51	0.62	0.43
Er	2.52	2.76	2.61	2.35	1.40	1.90	1.41
Tm	0.36	0.43	0.44	0.32	0.21	0.32	0.22
Yb	2.12	2.45	2.41	2.01	1.35	1.81	1.75
Lu	0.34	0.41	0.40	0.32	0.23	0.33	0.31
Fe_2O_3/MgO	2.5	2.4	6.8	2.5	3.2	2.6	11.0
$(La/Yb)_n$	7.79	7.15	8.85	9.34	11.20	8.19	8.44
$(La/Nd)_n$	2.00	2.13	2.49	2.45	2.64	2.45	3.48

Sample rock type	DC-15 Gr	DC-28 Gr	CN-1 Gr	CN-3 Gr	CN-10 Gr	CN12 Gr
SiO_2	70.71	76.62	77.12	73.25	77.81	73.51
TiO_2	0.50	0.11	0.13	0.21	0.12	0.22
Al_2O_3	14.35	12.42	12.65	13.62	12.51	13.74
Fe_2O_3	2.72	1.61	1.41	1.90	1.02	2.05
MnO	0.06	0.05	0.02	0.02	0.01	0.03
MgO	0.77	0.05	0.02	0.25	0.05	0.28
CaO	2.11	0.62	0.61	1.62	0.61	1.62
Na_2O	3.61	3.80	3.52	3.24	3.15	3.71
K_2O	4.52	4.51	4.90	4.71	5.31	3.91
P_2O_5	0.15	0.03	0.01	0.06	0.01	0.06
H_2O	0.30	0.30	0.31	0.51	0.42	0.61

(*continued on next page*)

Table 1 (*continued*)

Sample rock type	DC-15 Gr	DC-28 Gr	CN-1 Gr	CN-3 Gr	CN-10 Gr	CN12 Gr
Total	99.92	100.11	100.70	99.89	100.02	99.73
ASI	0.97	1.02	1.04	1.03	1.05	1.04
Co	0.11	0.32	0.61	0.50	0.60	0.55
Cr	40	134	28	19	30	23
Ni	19	27	24	20	16	22
Sr	302	38	8	127	22	235
Ba	566	218	10	262	16	443
Zr	224	112	101	133	99	106
Rb	211	180	291	264	351	150
Cs	4.71	4.07	12.32	17.60	9.20	4.49
Hf	0.89	2.52	2.41	4.71	3.11	3.51
Nb	10.5	11.5	11.1	6.2	4.1	7.5
Ta	1.12	1.32	1.19	1.20	2.52	1.10
Th	30.5	16.4	25.7	29.6	46.4	14.3
U	4.45	3.69	7.66	8.82	14.70	8.83
Y	26	29	51	48	76	24
Pb	16	17	29	34	28	26
Zn	44	37	40	46	30	31
La	42.7	19.3	19.7	29.1	38.6	22.6
Ce	82.4	41.5	45.6	59.8	77.5	44.0
Pr	8.80	4.80	5.81	6.98	10.90	4.91
Nd	30.8	17.7	24.0	26.5	40.0	17.7
Sm	5.32	3.89	6.50	6.14	8.87	3.81
Eu	1.01	0.32	0.11	0.50	0.31	0.50
Gd	4.20	3.61	6.32	5.82	6.59	3.31
Tb	0.51	0.52	1.04	1.01	0.87	0.52
Dy	3.22	3.30	6.68	6.31	4.76	3.21
Ho	0.61	0.71	1.40	1.32	0.90	0.75
Er	1.80	2.02	4.41	4.25	2.50	2.10
Tm	0.35	0.31	0.64	0.61	0.41	0.31
Yb	1.71	2.19	3.90	3.72	2.51	1.95
Lu	0.31	0.41	0.59	0.50	0.42	0.32
Fe_2O_3/MgO	3.5	32.0	70.0	7.6	20.0	7.1
$(La/Yb)_n$	16.80	6.87	3.31	5.20	10.32	7.83
$(La/Nd)_n$	2.65	2.09	1.54	2.10	1.85	2.45

Rock types: Granodiorite (GrD); Granite (Gr); ASI = aluminum saturation index (molar $Al_2O_3/(CaO + K_2O + Na_2O)$), Co is normative corundum, and total iron is expressed as Fe_2O_3.

4. Results

4.1. Major and trace element geochemistry

Representative chemical analyses of samples are listed in Table 1. The bulk-rock concentrations of the Dalat granitoids are characterized by high SiO_2 and low MgO, and very low abundances of high-field strength elements (Nb, Ta, Zr and Hf). For example, Nb is generally lower than the average value of I-type (14 ppm) and felsic I-type (21 ppm) granites in the Lachlan Belt of southeastern Australia (Chappell and White, 1992; Chappell, 1999). In some highly fractionated I-type granites, however, the Nb contents can reach up to ~40 ppm (Fig. 5e). In terms of normative mineralogy, the Dinhquan granitoids have, except for one sample, granodioritic compositions (Fig. 2). In contrast, most of the Cana and Deoca granitoids approach minimum melt compositions. The A/CNK vs. A/NK diagram (Maniar and Piccoli, 1989) defines the rocks as metaluminous to slightly peraluminous, and of I-type character (Fig. 3a). All samples are of subalkaline affinity and belong to the calc-alkaline series. The K_2O vs. SiO_2 plot further shows almost all samples to be of high-K affiliation (Fig. 4f).

Major and trace element variations are illustrated in Harker diagrams in Figs. 4 and 5. The samples exhibit a wide range in SiO_2 content from approximately 56 to 70 wt% for the Dinhquan, 64 to 77 wt% for the Deoca, and 70 to 78 wt% for the Cana suites. TiO_2, Al_2O_3, Fe_2O_3, MgO, CaO, and P_2O_5 abundances decrease with increasing SiO_2, whereas K_2O increases and Na_2O remains nearly constant. The trace elements (Fig. 5) exhibit considerably more scatter than the major elements, particular Ba and Zr. However, Sr shows a negative linear trend, whereas Rb defines a positive correlation with increasing SiO_2 contents. Although rocks of all three suites exhibit typical high-K, calc-alkaline compositions, the variation diagrams reveal some differences among them (Figs. 4 and 5). The Cana

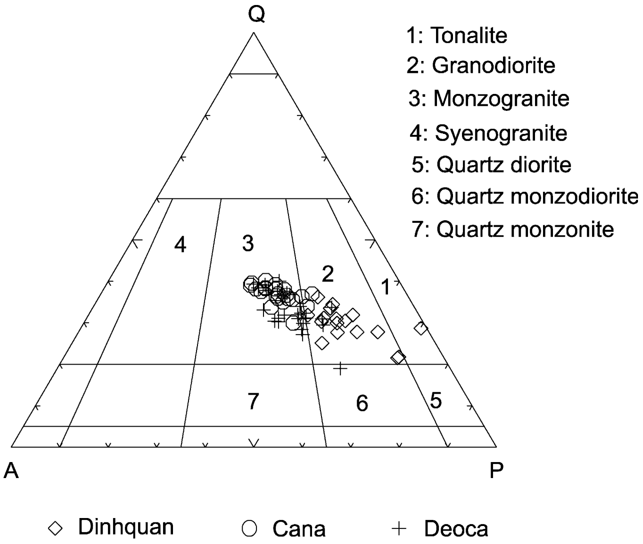

Fig. 2. Ternary diagram illustrating the compositions of the Dalat zone granitoids. Nomenclature taken from Le Maitre (1989): quartz (Q)–alkali feldspar (A)–plagioclase (P).

rocks exhibit a higher and smaller range in SiO_2 content. Among the trace elements, samples of the Deoca suite have more scattered Ba and Zr patterns than those from the Dinhquan and Cana suites.

4.2. Rare earth element geochemistry

Chondrite-normalized REE patterns are plotted in Fig. 6. The REE patterns of all analyzed samples from the three suites are characterized by fractionation between the light and heavy REEs. The Dinhquan samples exhibit moderately fractionated REE patterns ($[La/Yb]_{n=}$8–11), flat heavy REE patterns, and have slight or no Eu anomalies ($Eu/Eu^* = 0.55 - 0.97$). The Cana samples are characterized by variably fractionated and flatter heavy REE patterns ($[La/Yb]_n = 3–10$) and have strong negative Eu-anomalies ($Eu/Eu^* = 0.04–0.39$). The Deoca samples have strongly fractionated REE patterns ($[La/Yb]_n = 7–17$) with small to large negative Eu anomalies ($Eu/Eu^* = 0.25–0.67$). Most of the Deoca rocks are characterized by depletion of the middle REEs (Gd to Er) relative to other HREEs. Primitive mantle-normalized spidergrams from all three suites show enrichment in large ion lithophile (LIL) elements (e.g. Cs, Rb, Th, K, and U) and exhibit distinct negative anomalies for high field strength (HFS) elements (Nb and Ti) (Fig. 7). Noteworthy is the decoupling of Ba and Sr from Rb and K as shown by negative Ba and Sr spikes.

4.3. Nd–Sr–O isotopic ratios

Samples for Nd, Sr, and O isotope analyses were chosen to cover the entire compositional spectrum of the three suites, from the most primitive through to most evolved members. The data are given in Table 2 and Fig. 8. Nd isotopic compositions were calculated for ages of 110 My (Dinhquan), 96 My (Cana), and 92 My (Deoca). These ages were obtained from conventional U–Pb zircon geochronology and are interpreted to represent the emplacement ages of the granitoids (Thuy Nguyen et al., 2000). However, one extremely high $^{87}Rb/^{86}Sr$ ratio (107.15) of a Cana sample (C N-1), either caused by secondary Rb enrichment and/or Sr loss, has been excluded from the initial Sr calculation, as it would lead to a geologically meaningless value of the initial $^{87}Sr/^{86}Sr$ isotopic ratio. Nd and Sm are much less mobile than Sr and Rb, and Nd isotopic ratios are, particularly for the sample C N-1, more reliable source indicators. Fig. 8a shows the variation of initial $^{143}Nd/^{144}Nd$ expressed as

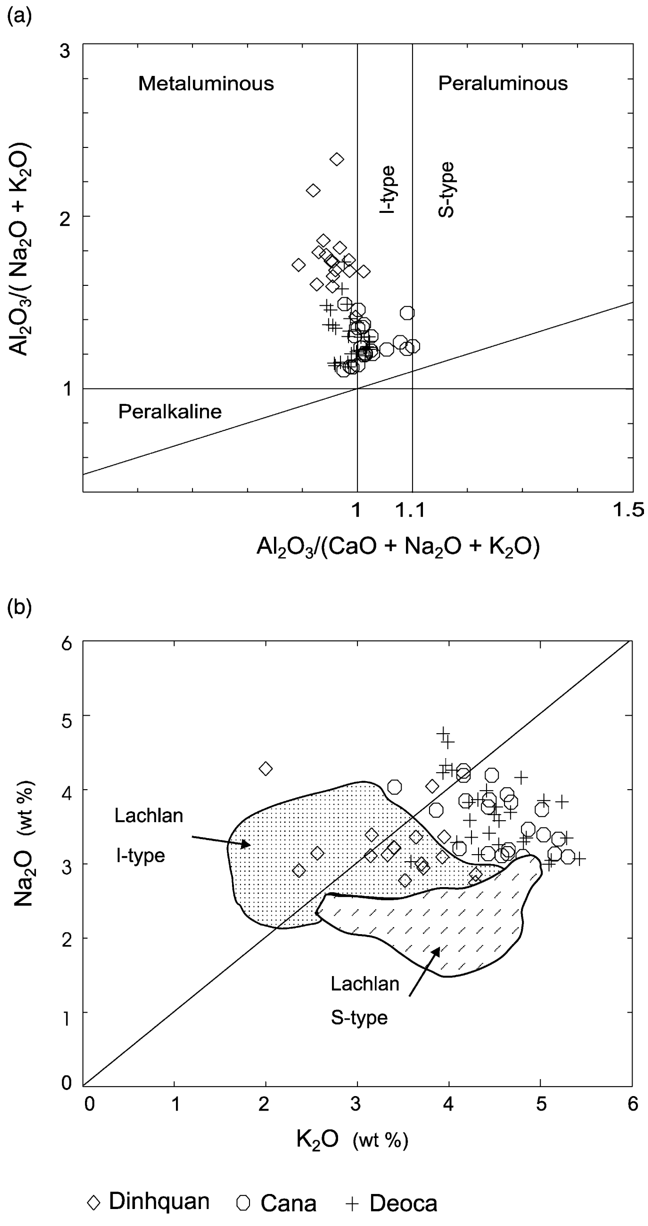

Fig. 3. (a) a plot of Shand's index for granitoids in the Dalat zone. Discrimination fields for different types of granitoids (Maniar and Piccoli, 1989 Shand, S.J., 1927) are shown; (b) a plot of Na_2O vs. K_2O (wt%). I- and S-type granitoids of the Lachlan Fold Belt are shown for comparison (White and Chappell, 1983).

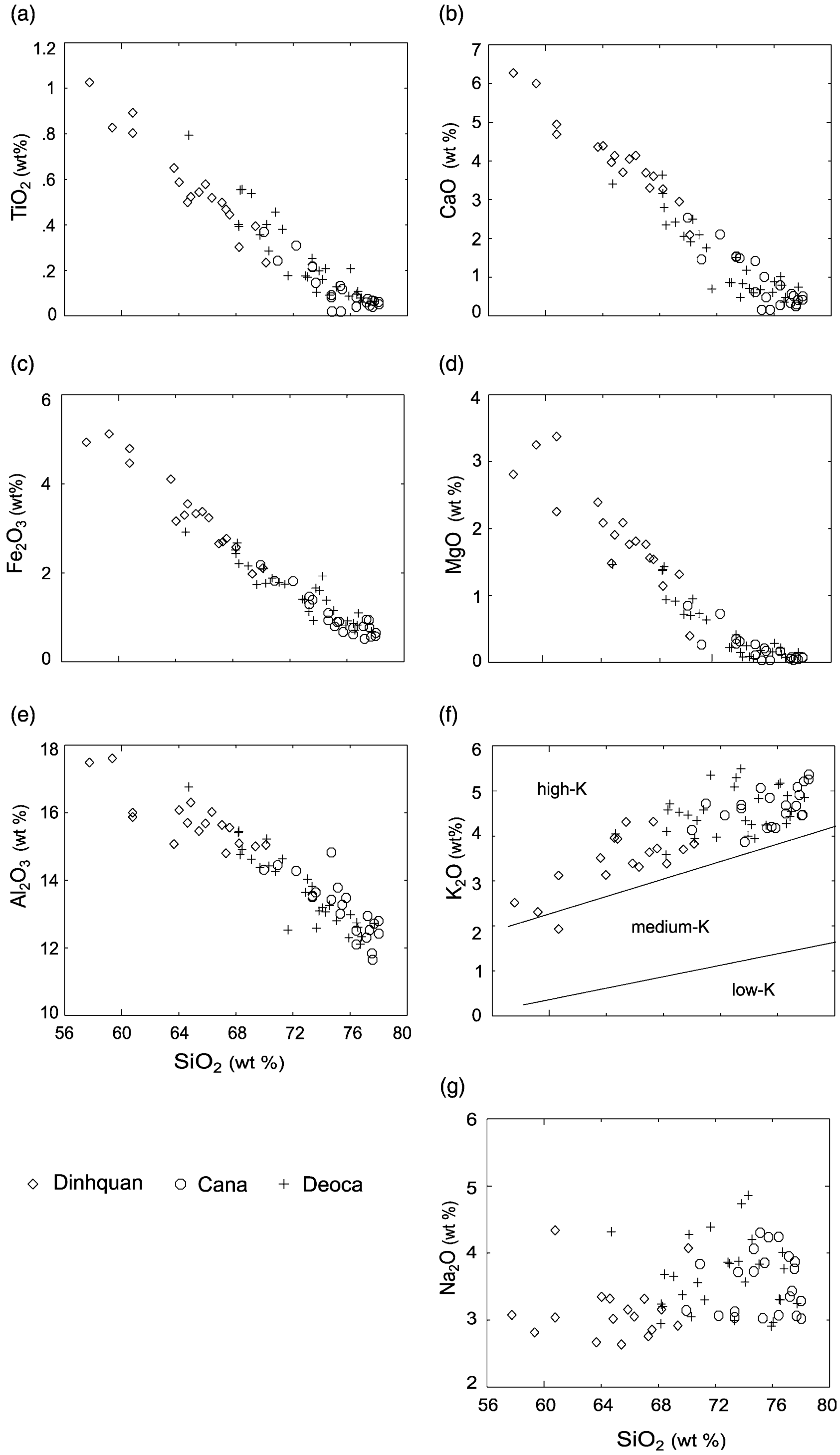

Fig. 4. (a–g) Selected Harker variation diagrams of major elements for the Dalat zone granitoids. The K_2O vs. SiO_2 diagram (Fig. 4f) after Le Maitre (1989) with lines separating low-K, medium-K, and high-K granites.

$\varepsilon_{Nd(T)}$ values with initial $^{87}Sr/^{86}Sr$ (Sr_i) isotopic ratios. Taken as a whole, the Dinhquan and Deoca samples have a pronounced negative correlation between both parameters, whereby $\varepsilon_{Nd(T)}$ values decrease with increasing Sr_i values. The three Cana samples have nearly constant $\varepsilon_{Nd(T)}$ with slightly increasing Sr_i. The important point to note from this figure is that the Deoca samples have a wide range of both Sr and Nd isotopic ratios, ranging from less radiogenic to more radiogenic isotopic compositions. Three of four Dinhquan samples are displaced to lower Sr isotope ratios compared to the Cana and Deoca samples.

The $\delta^{18}O$ values, except for some samples having $\delta^{18}O$ values lower than 7.5‰, which were likely affected by hydrothermal alteration, range from 7.5 to 8.9‰. These

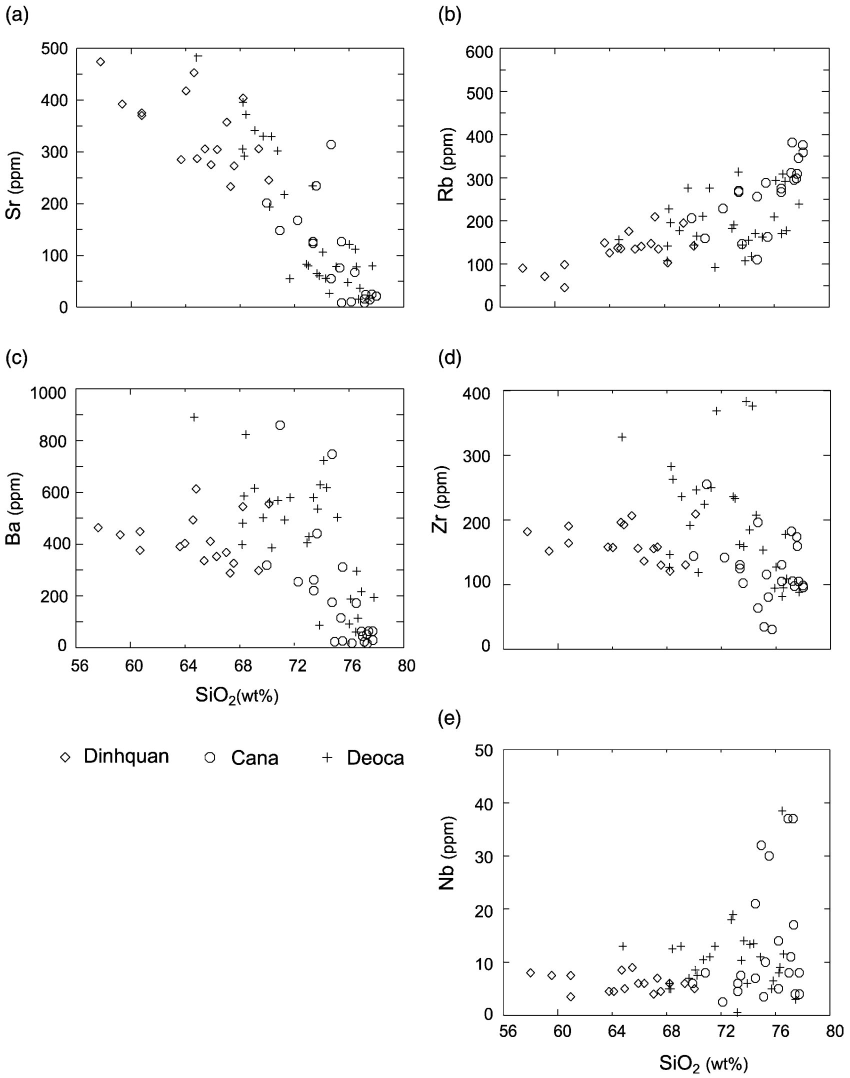

Fig. 5. (a-e) Selected Harker variation diagrams of trace elements for the Dalat zone granitoids.

latter values are typical for 'normal' granites (Taylor, 1968; O'Neil and Chappell, 1977). A slightly positive correlation between $\delta^{18}O$ values and SiO_2 is observed for the Dinhquan and Cana samples (Fig. 8b). Such a trend, however, does not exist for samples of the Deoca suite. It is noteworthy that with SiO_2 content <76 wt%, the Deoca samples tend to have lower $\delta^{18}O$ values compared to samples having similar SiO_2 content from the Cana suite.

5. Discussion

5.1. Petrogenetic considerations

Petrogenetic models for the origin of felsic arc magmas fall into two broad categories. In the first, felsic arc magmas are derived from basaltic parent magmas by fractional crystallization or AFC processes (e.g. Grove and Donnelly-Nolan, 1986; Bacon and Druitt, 1988). The second model is that basaltic magmas provide heat for the partial melting of crustal rocks (e.g. Bullen and Clynne, 1990; Roberts and Clemens, 1993; Tepper et al., 1993; Guffanti et al., 1996). The first model is considered to be unlikely, because volcanic and granitoid rocks of the Dalat zone are voluminous and none are of basaltic composition (all samples have SiO_2 content $>56\%$, Fig. 5). Such voluminous felsic magmas could not be generated by differentiation of mantle-derived mafic magmas. Furthermore, the rock compositions do not represent a fractionation sequence from basalt to granodiorite or leucogranite. Rocks of all three suites show little variation in initial Sr-isotope ratios and $\delta^{18}O$ values with SiO_2 (Fig. 8b and c), which does not support derivation from mafic magmas through AFC processes. It is also unlikely that the granitoids represent mixtures of basaltic and granitic magmas, as coeval basaltic members are lacking in the Dalat zone. There is abundant experimental evidence that hydrous melting of basalt could produce tonalitic-trondhjemitic magmas (e.g. Wyllie, 1984) that might evolve (by fractionation and/or crustal contamination) toward more granitic compositions. Tepper et al.

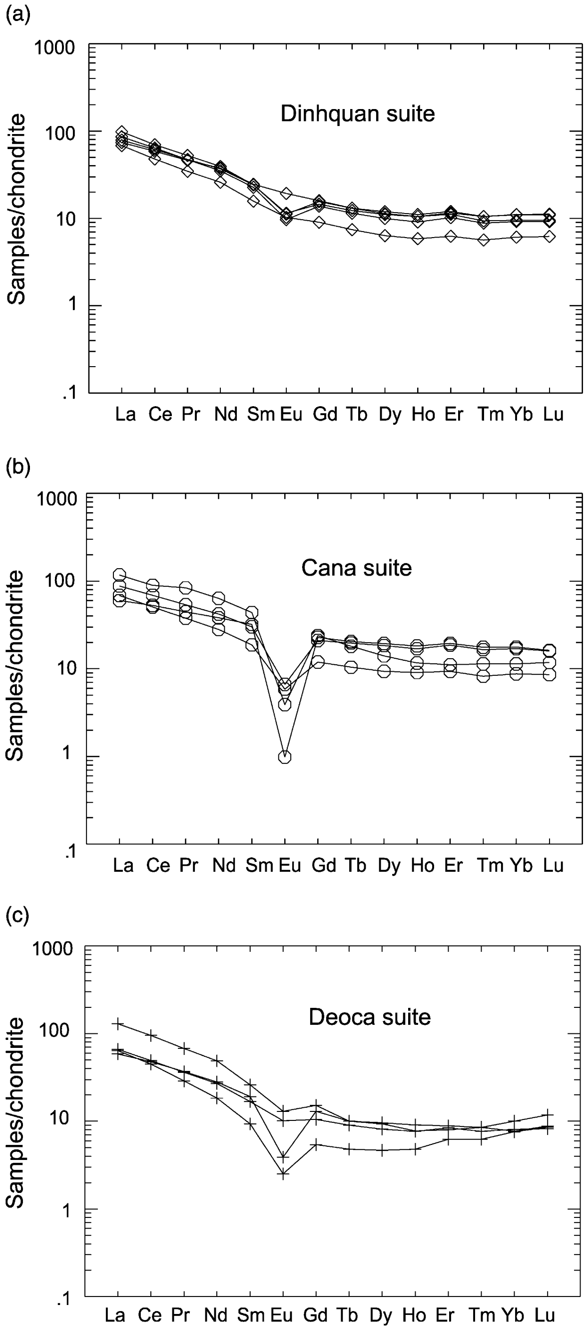

Fig. 6. (a-c) Chondrite-normalized rare earth element abundances for the Dalat zone granitoids (normalizing values from Sun, 1982).

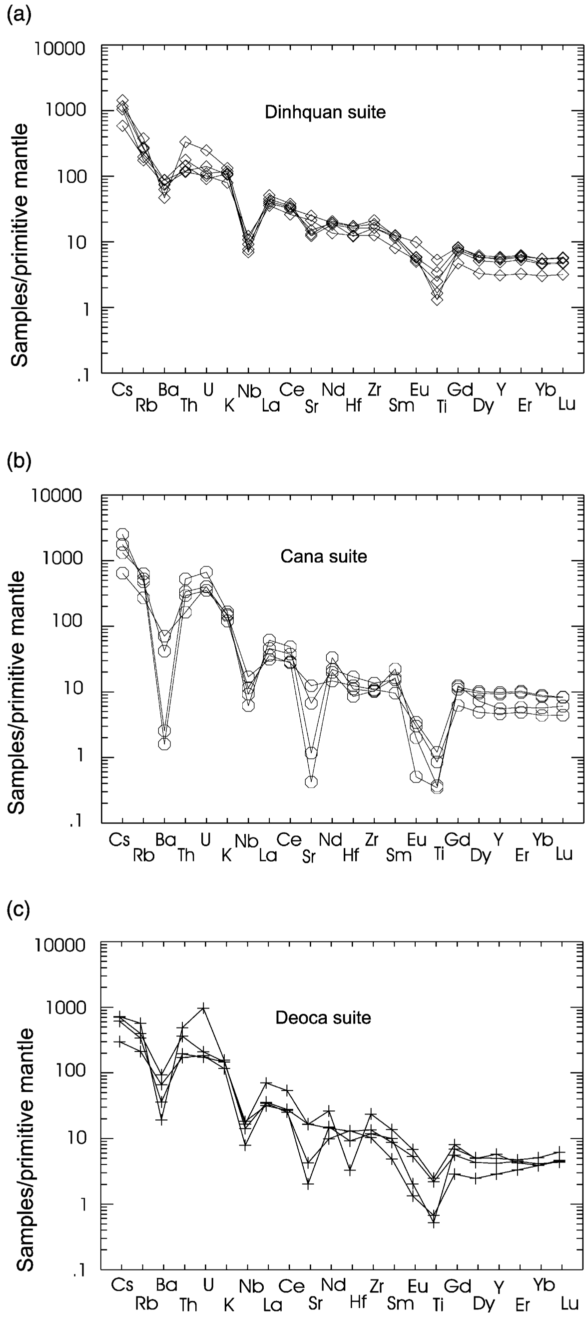

Fig. 7. (a–c) Primitive mantle-normalized trace element abundances for the Dalat zone granitoids. The normalizing values are from Taylor and Mclennan (1985).

(1993) reported that partial melting of lower crustal metabasalt yields a variety of granitoids, whose compositions were controlled by variation in H_2O content. A similar conclusion was reached by Jonasson (1994) for the origin of rhyolite from Iceland. Roberts and Clemens (1993), on the basis of the data on the experimental partial melting of common crustal rocks, stated that high-K, I-type, calc-alkaline granitoid magmas can be derived from the partial melting of hydrous, calc-alkaline mafic to intermediate metamorphic rocks in the crust. Given the available experimental constraints, we think that the most reasonable model for the origin of the Dalat granitoids involves partial melting of crustal protoliths having different compositions, leaving restites with variable proportions of amphibole and plagioclase as a result of melting under variable H_2O contents. Mantle-derived basaltic magmas emplaced into the lower crust are the most likely heat sources for partial melting. Fractional crystallization of the melts en route to higher crustal levels can generate the whole spectrum of granitoid types represent in the Dalat zone. Upper crustal contamination did not play an important role in

Table 2
Sm–Nd, Rb–Sr and O isotopic data of granitoids from the Dalat zone

Sample	Sm (ppm)	Nd (ppm)	$(^{147}Sm/^{144}Nd)$	$(^{143}Nd/^{144}Nd) \pm 2\sigma m$	$\varepsilon_{Nd(T)}$	T_{DM}	$^{87}Rb/^{86}Sr$	$(^{87}Sr/^{86}Sr) \pm 2\sigma m$	$(^{87}Sr/^{86}Sr)_i$	$\delta^{18}O$ (‰)
CN-1[a]	6.50	24.0	0.1628	0.512486 ± 11	−2.5	1.65	107.15	0.89376 ± 12	0.74131	8.9
CN-3	6.14	26.5	0.1384	0.512464 ± 10	−2.7	1.16	6.02	0.71468 ± 10	0.70636	8.9
CN-10	8.87	40.0	0.1329	0.512470 ± 11	−2.5	1.08	46.44	0.77030 ± 11	0.70615	8.7
CN-12	3.81	17.7	0.1278	0.512462 ± 10	−2.5	1.03	1.85	0.70857 ± 10	0.70601	6.7
DC-3	3.42	17.0	0.1203	0.512517 ± 10	−1.5	0.86	1.07	0.70758 ± 11	0.70618	5.9
DC-10	1.90	11.6	0.0961	0.512406 ± 10	−3.3	0.83	11.20	0.72161 ± 10	0.70699	8.9
DC-15	5.32	30.8	0.1052	0.512431 ± 10	−2.9	0.86	2.02	0.70932 ± 10	0.70668	8.0
DC-28	3.89	17.7	0.1340	0.512645 ± 10	+0.9	0.77	13.87	0.72364 ± 10	0.70554	7.8
DQ-6	4.92	23.3	0.1302	0.512512 ± 10	−1.5	0.97	1.55	0.70749 ± 10	0.70510	7.4
DQ-7	4.91	24.8	0.1143	0.512479 ± 10	−2.0	0.87	1.72	0.70805 ± 11	0.70539	8.2
DQ-8	4.62	22.1	0.1179	0.512541 ± 10	−0.8	0.80	2.61	0.70901 ± 10	0.70498	8.9
DQ-12	3.21	16.3	0.1217	0.512513 ± 11	−1.4	0.88	0.78	0.70734 ± 10	0.70614	7.3

m = measured isotopic ratios; i = calculated initial isotopic ratios. $\varepsilon_{Nd(T)}$ values were calculated using present day $(^{143}Nd/^{144}Nd)_{CHUR} = 0.512638$ and $(^{147}Sm/^{144}Sm)_{CHUR} = 0.1967$ (CHUR = chondritic uniform reservoir; $\lambda = 6.54.10^{-12}$ a^{-1}). The ages of 110 My (Dinhquan), 96 My (Cana) and 92 My (Deoca) are used for $\varepsilon_{Nd(T)}$ and $(^{87}Sr/^{86}Sr)_i$ calculations; $[(^{87}Sr/^{86}Sr)i = (^{87}Sr/^{86}Sr)m - ^{87}Rb/^{86}Sr\ (e^{\lambda t} - 1);\ \lambda = 1.42.10^{-11}\ a^{-1}]$.

[a] Sample C N-1 is highly fractionated granite and therefore has old T_{DM}. If a correction is made using typical crustal $^{147}Sm/^{144}Nd$ ratio = 0.12, the resulting T_{DM} of 1.07 Ga is more realistic.

the formation of granitoids in the Dalat zone. Because the basement underlying the Dalat zone is not exposed, it is difficult to evaluate the role of the basement in the origin of the Dalat zone granitoids. Nevertheless, their parental magma characteristics, potential sources and crystallization behavior within an individual suite can be constrained by the geochemical and isotopic data.

5.2. Fractional crystallization

Increases in SiO_2, K_2O, Rb, and decreases in TiO_2, Fe_2O_3, CaO, MgO and Al_2O_3 contents shown in each granitoid suite are compatible with their evolution through fractional crystallization processes (Figs. 4 and 5). Strongly negative Ba and Sr anomalies in rocks from the Cana and Deoca suites are associated with negative Eu anomalies, indicating evolution by fractionation of K-feldspar and plagioclase either in magma chambers or during magma ascent. This is also supported by negative correlations between CaO, Al_2O_3, and SiO_2 (Fig. 4). In contrast, fractionation of plagioclase has not played an important role in the petrogenesis of the Dinhquan granitoids, as indicated by small or no negative anomalies of Eu, Ba, and Sr (Figs. 6 and 7). Decreases in TiO_2 and P_2O_5 with increasing SiO_2 content are attributed to fractionation of titanite and apatite, respectively. The fractionation of accessory phases such as zircon, allanite and titanite can account for depletion in zirconium and yttrium. The Deoca samples display moderate concave upward REE patterns and relative depletion of middle REEs with respect to HREEs (Fig. 6c), which can be attributed to fractionation of hornblende and/or titanite (e.g. Romick et al., 1992; Hoskin et al., 2000). The Cana granites have high SiO_2 contents and some of them have very high values of Fe_2O_3/MgO ratios (Table 1), indicating that parental magmas for the Cana granites have experienced extensive magmatic differentiation (Whalen et al., 1987). Some samples were affected by hydrothermal alteration, as indicated by their very high values of K/Ba (840–2750) and low K/Rb (120–1300) ratios.

The $\delta^{18}O$ values range from 5.9 to 8.9‰ (Fig. 8b). The samples from all three suites with $\delta^{18}O$ values less than 7.5‰ probably reflect meteoric-hydrothermal alteration at some stage after their emplacement. Evidence for this is turbidity of feldspars and biotites are partly replaced by chlorite. Except for those altered samples, an increase in $\delta^{18}O$ values of about 1‰ throughout the Dinhquan suite and about 0.8‰ throughout the Cana suite may be attributed to fractional crystallization without significant contamination by continental crust, since closed-system fractional crystallization is known to modify $\delta^{18}O$ values by about 0.5–1‰ (e.g. Taylor, 1978; Woodhead et al., 1987; Harmon and Gerbe, 1992). The wider range in $\delta^{18}O$ values (7.7–8.9‰) of the Deoca samples may reflect an inhomogeneous source.

The continuous chemical variations illustrated in Harker diagrams (Figs. 4 and 5) and the close spatial and temporal association of granitoids from all three suites, suggest that these granitoids may be linked through differentiation from the same magmatic source. To elucidate this problem, variation diagrams of the concentrations of some selected oxides and elements, which are strongly affected by fractional crystallization process, have been plotted against Mg# (Fig. 9). It is evident that the crystallization behavior between the Dinhquan and Cana suites is different. Except for Mg# < 30, the Cana samples have well-defined trends whereby TiO_2, P_2O_5, MgO, CaO, and Sr decrease with decreasing Mg#. In contrast, the Dinhquan samples do not follow these trends. Nd model ages (T_{DM}) of granitoids range from 1.03 to 1.16 Ga for the Cana, 0.77 to 0.86 Ga for the Deoca, and 0.80 to 0.97 Ga for the Dinhquan suites. The Cana granites have distinctly older T_{DM} than the others two, suggesting that they were derived from separate magmas or

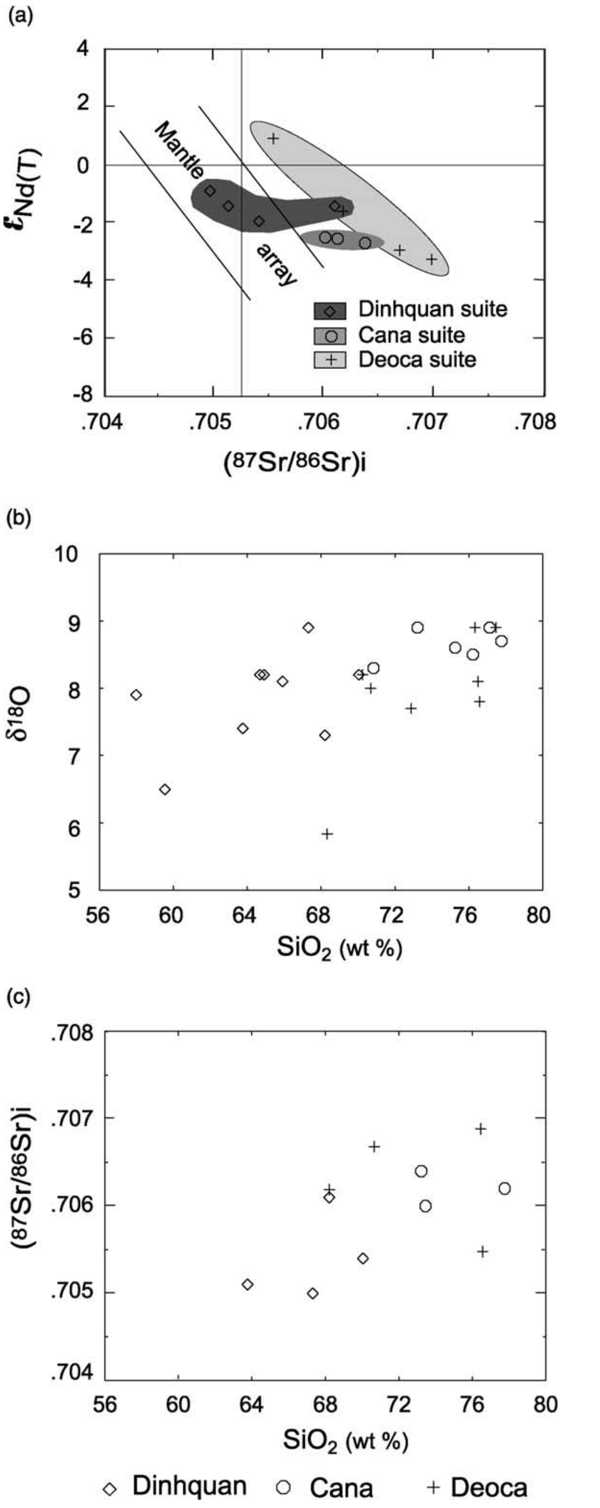

Fig. 8. (a–c) Nd, Sr, and O isotopic compositions of selected samples from all three suites of the Dalat zone granitoids; (a) initial $\varepsilon_{Nd(T)}$ values vs. initial Sr isotopic ratios; (b) and (c) $\delta^{18}O$ values and initial Sr isotopic ratios vs. SiO_2, respectively.

underwent different petrogenetic processes. Therefore, a comagmatic and continuous crystal fractionation relationship between the Cana and other two suites is unlikely. The slightly higher HREE concentrations, lower $(La/Yb)_n$ and $(La/Nd)_n$ ratios but higher SiO_2 of the Cana samples (Table 1) argue against a co-genetic relationship through crystal fractionation and indicate that the Dinhquan and Cana sources were chemically distinct.

The Deoca samples, in spite of some scatter, generally exhibit coherent trends for most elements, but display considerable variation in Mg#. Differentiation of the Dinhquan or Cana parent magmas alone to produce the Deoca granitoid rocks is excluded because the samples have overlapping Mg#. The initial Nd and Sr isotopic compositions of the Deoca samples lie outside the range of Dinhquan and Cana rocks (Fig. 8a) and the concentration of trace elements (e.g. Ba, Sr, and Zr) do not fall on a straight line between the Dinhquan and Cana samples in Harker variation diagrams (Fig. 5). Furthermore, rocks of the Deoca suite are pink to red and exhibit porphyritic textures, which are not observed for the Dinhquan and Cana rocks. All these features suggest that magma mixing of Dinhquan and Cana also cannot produce the Deoca rocks, hence a different magmatic source is proposed for the Deoca granitoids.

5.3. Nature of parental magmas and potential sources

Granitoids of all three suites are high-K, calc alkaline rocks and are characterized by pronounced negative Ba, Sr, Nb, and Ti anomalies and are enriched in Rb, Th, K, and La. These features are compatible to those of typical crustal melts, e.g. granitoids of the Lachlan Fold belt (Chappell and White, 1992) and Himalayan leucogranites (Harris et al., 1986; Searle and Fryer, 1986). Hence a derivation from crustal sources is apparent. The crustal source rocks are not exposed in the Dalat zone but they are probably mid-Proterozoic in age, as indicated by U–Pb inherited zircon ages (e.g. Thuy Nguyen et al., 2002; Carter et al., 2001; Nagy et al., 2001; Nam et al., 2001). Compositional diversity among crustal magmas may arise in part from different source compositions, in addition to variation in melting conditions such as H_2O contents, pressure, temperature, and oxygen fugacity. (e.g. Vielzeuf and Holloway, 1988; Wolf and Wyllie, 1994; Patĩno Douce, 1996, 1999; Thompson, 1996; Borg and Clynne, 1998). Compositional differences of magmas produced by partial melting under variable melting conditions of different crustal source rocks such as amphibolites, gneisses, metagraywackes and metapelites, may be visualized in terms of major oxide ratios. Partial melts originating from mafic source rocks, for example, have lower Al_2O_3/(FeOtotal + MgO + TiO_2) and (Na_2O + K_2O)/(FeOtotal + MgO + TiO_2) than those derived from metapelites (Fig. 10). The Dinhquan rocks have lower values of Al_2O_3/(FeOtotal + MgO + TiO_2), (Na_2O + K_2O)/(FeOtotal + MgO + TiO_2) and a rather high and narrow range of CaO/(FeOtotal + MgO + TiO_2) ratios compared to Cana and Deoca rocks. These features, in combination with relatively high values of Mg# (68–38), preclude a derivation from felsic pelite and metagreywacke rocks for the Dinhquan granitoids. Instead, the Dinhquan

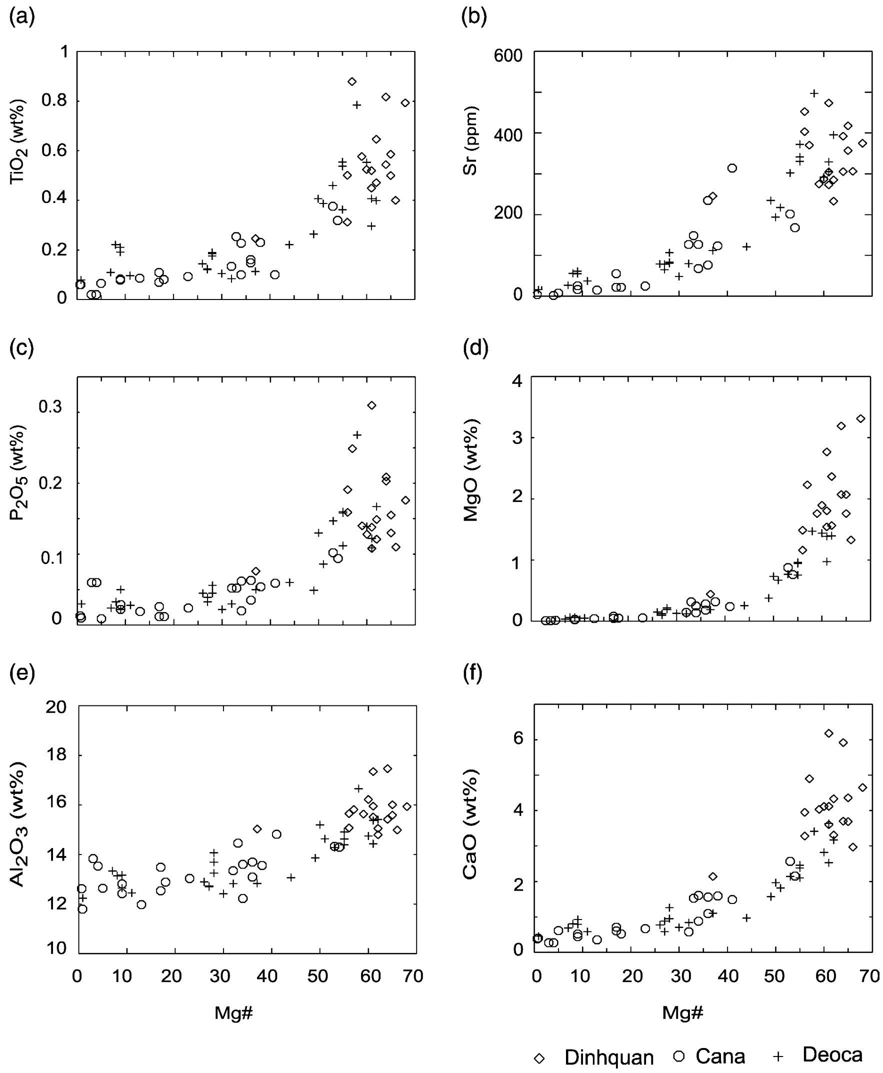

Fig. 9. (a–f) Variation diagrams of selected oxides and elements vs. Mg# for the Dalat zone granitoids. Mg# [= 100xmolar MgO/(MgO + $0.9FeO_{tot}$)].

magmas were generated by partial melting of alkaline mafic lower crustal source rocks. On the Na_2O vs. K_2O diagram (Fig. 3b), most of the Dinhquan samples plot in the field outlined for typical I-type granite of the Lachlan Fold Belt (White and Chappell, 1983). High contents of CaO, Sr, and negligible Eu/Eu* depletion in the REE patterns all suggest melting of a plagioclase-bearing source. Less fractionated REE- and flat HREE patterns suggest that the role of garnet in the crustal precursor was not important.

Compared to typical Lachlan S-type granites (White and Chappell, 1983), the Cana and Deoca rocks have much higher Na_2O but similar K_2O contents (Fig. 3b) and lower A/CNK ratios. The fact that granitoids of both suites are compositionally transitional between Lachlan I-and S-type granites implying that the Cana and Deoca granitoids might have been derived from partial melting of acid to intermediate igneous rocks or immature sediments. All plots in Fig. 10 indicate an origin of the Cana and Deoca magmas by dehydration melting of metagreywacke-type source rocks. Some of the Cana granites fall in the range of felsic pelite (Fig. 10b), as these samples contain secondary muscovite. Muscovitization of feldspar and chloritization of biotite in these samples suggest hydrothermal alteration. Excluding C N-1, the Cana granites have a narrow range of initial Sr-isotope ratios (0.7060–0.7064) and nearly constant $\varepsilon_{Nd(T)}$ values (−2.5 to −2.7) (Fig. 8a), indicating derivation from a rather homogeneous melt that underwent closed-system fractional crystallization as demonstrated by the $\delta^{18}O$ values of granites. These granites yield Nd model ages ranging from 1.03 to 1.16 Ga which are a little younger than basement ages but similar to inherited zircon ages found in one of their granites (Thuy Nguyen et al., 2002). This emphasizes that crustal material played a very important role in their petrogenesis. Furthermore, the granites show strong depletion in Sr (Fig. 7) and Eu/Eu* (Fig. 6) ratios reflecting melting with residual plagioclase and/or plagioclase as a major fractionating phase. None of the Cana granites show the HREE depletion predicted for melts that equilibrated with residual garnet (Tepper et al., 1993).

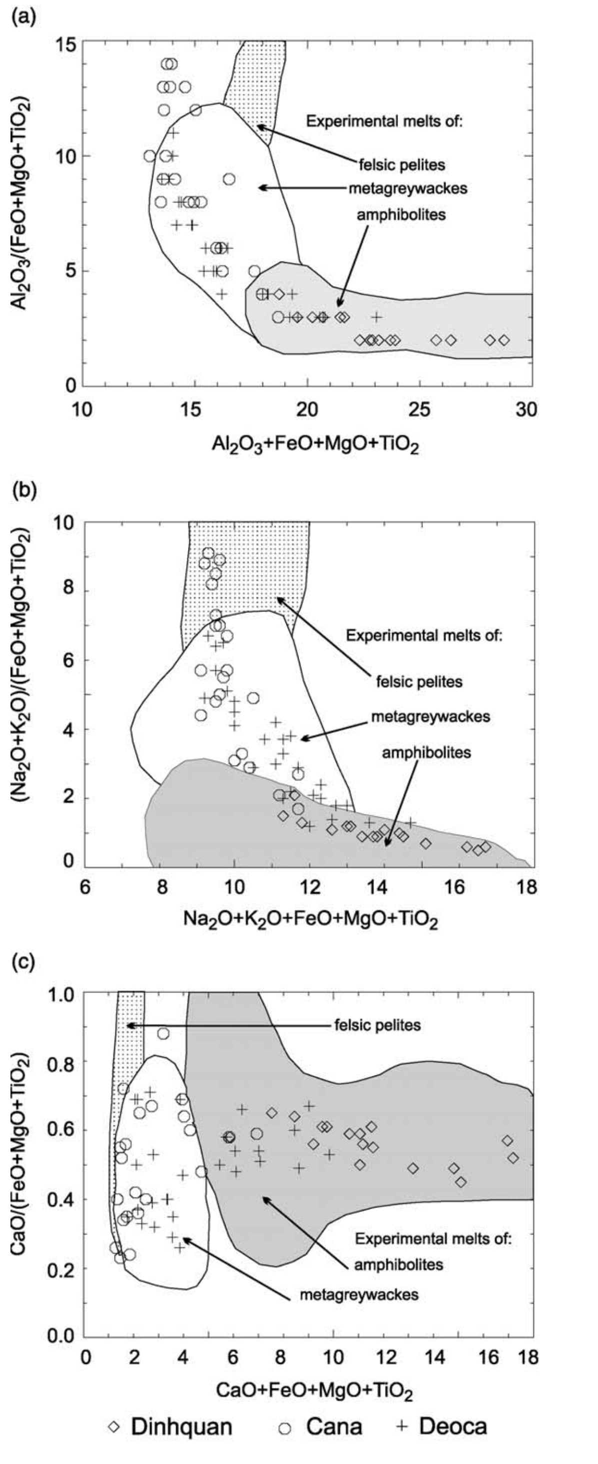

Fig. 10. (a–c) Plots show compositional fields of experimental melts derived from partial melting of felsic pelites, metagreywackes and amphibolites (Patĩno Douce, 1999) and compositions of studied samples. See text for discussion.

In contrast to Cana granites, the Deoca samples show relatively large variations in isotopic compositions ($\varepsilon_{Nd(T)} = \sim 1$ to ~ -3; $Sr_i = 0.7055–0.7069$) suggesting their derivation from heterogeneous sources. The slightly negative to weakly positive $\varepsilon_{Nd(T)}$ values, low Sr_i ratios, and young Nd model ages ($T_{DM} = 0.77–0.86$ Ga) indicate significant input of a mantle-derived component during magma generation. Therefore, a mixture of juvenile material and old continental crust may characterize the petrogenesis of these granitoids. In this case, Nd model ages represent the average crustal residence time for the Deoca granitoids (Jahn et al., 1990). Compared with the Cana rocks, the Deoca rocks have higher values of Eu/Eu* and higher abundances of Sr suggesting a smaller amount of plagioclase in their residues during magma segregation. Furthermore, the rocks show the concave-upward REE patterns and are depleted in MREE relative to HREE (Fig. 6c) indicating that amphibole played a dominant and garnet an insignificant role during magma segregation. The MREE depletion and the negative Ti anomaly can also be attributed to fractional crystallization of titanite (e.g. Weaver, 1990; Hoskin et al., 2000) as we found this mineral in some Deoca samples.

It is worth to note that not all granitoids in the world fit into alphabetical classification of Chappell and White (1974), as reported by Patĩno Douce (1999). The same conclusion is reached by Barker et al. (1992) that the generation of Alaskan granitoids by melting of flyschoid sediments mainly consisting of greywackes and the finer-grained argillite, nevertheless, they typically show I-type characters. A further support for the derivation of high-potassium, calc-alkaline I-type granitoids in northern Schwarzwald (Germany) from metagreywackes is achieved by Altherr et al. (2000). Thus, perhaps particularly relevant is that the Cana and Deoca granitoids derived from metagreywacke-type source rocks have been shown to exhibit I-type geochemical characteristics similar to those in Alaska and northern Schwarzwald. Probably the geochemical features of the Cana and Deoca granitoids reflect largely the igneous parentage of these metagreywackes.

5.4. Tectonic setting: evidence for continental arc magmas

Granitoids of all three suites are high-K, calc alkaline rocks enriched in LILEs such as Cs, K, Rb, U and Th with respect to the HFSEs, especially Nb and Ti (Fig. 7). Magmas with these chemical features are generally believed to be generated in subduction-related environments (e.g. Floyd and Winchester, 1975; Rogers and Hawkesworth, 1989; Sajona et al., 1996). Numerous studies suggest that trace elements could be used as discriminatory tools to distinguish among different tectonic settings of granitoid magmas. Pearce et al. (1984) used the Rb, Y, and Nb elements as the most efficient discriminants amongst ocean-ridge granites (ORG), within-plate granites (WPG), volcanic-arc granites (VAG) and syn-collisional granites (syn-COLG). Applying their discrimination criteria, the Dalat zone granitoids are classified as VAG (Fig. 11a). These VAG belong to the group of 'active continental margin' rocks (Group C after Pearce et al., 1984). They contain biotite and hornblende, are metaluminous to weakly peraluminous, and have the characteristics of I-type granites (White and

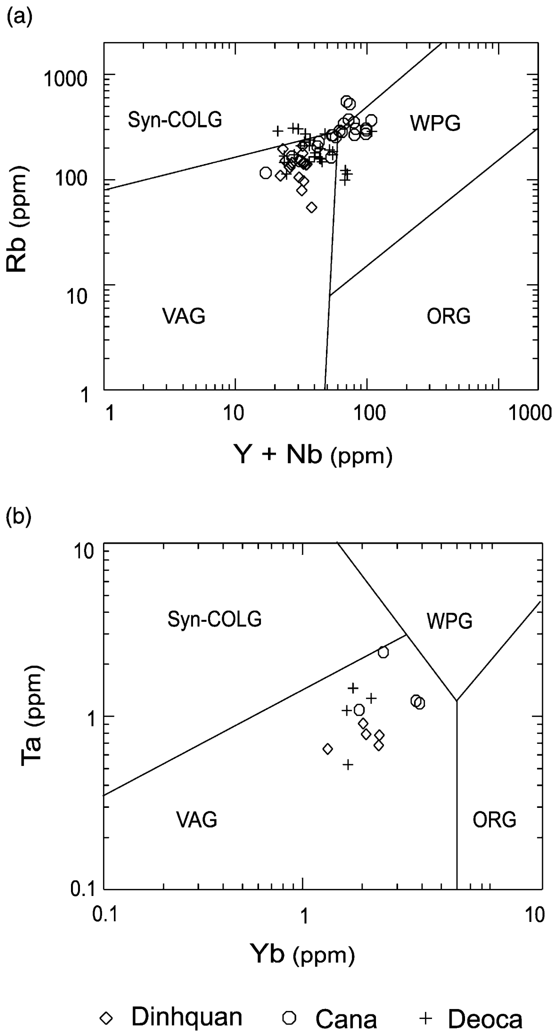

Fig. 11. (a–b) Chemical compositions of the Dalat zone granitoids in the Rb vs. (Y + Nb) and Ta vs. Yb discrimination diagrams of Pearce et al. (1984). Abbreviations: VAG, volcanic-arc granitoids, syn-COLG, syn-collisional granitoids, WPG, within plate granitoids, ORG, ocean-ridge granitoids.

Chappell, 1983; Chappell and White, 1992). The high-silica samples (75–77 wt% SiO_2) from the Cana suite plot around the boundary between the COLG and WPG field, but lower-silica samples (70–74 wt% SiO_2) fall within the VAG field (Fig. 11a). This is likely due to progressive differentiation (Förster et al., 1997). Crossing of the VAG and COLG boundary, as is observed for some Deoca samples, is the result of a magmatic differentiation trend. On the Ta vs. Yb diagram (Pearce et al., 1984; Fig. 11b) all analyzed samples fall into the VAG field. Further arguments in favor of volcanic arc characteristics for the Dalat zone granitoids come from their Rb/Zr and Rb/Cs values. Similar to arc magmas reported by Hart and Reid (1991), all the Dalat zone granitoid samples display low ratios of Rb/Cs (<30 for the Dinhquan, <40 for the Cana and <60 for the Deoca samples). Low values of Rb/Zr ratios (<1.3) in almost all samples, with some granites from the Cana suite having slightly higher values (up to 3.5), are also compatible with volcanic arc settings (Harris et al., 1986). Note that trace element compositions of magmas are also dependent on protolith composition and, therefore, may not necessarily be indicative of the tectonic setting of magma formation (e.g. Roberts and Clemens, 1993). However, the spatial and temporal relationship of the Dalat zone granitoids, in conjunction with their geochemical and mineralogical data, indicates a subduction-related origin.

6. Conclusions

The Dalat zone granitoids have I-type characteristics and belong to the high-K calc-alkaline series. The geochemical and isotopic compositions of Dinhquan granitoids indicate derivation by dehydration melting of alkaline mafic lower crustal source rocks, while the Cana magmas were generated from a relatively homogeneous metagreywacke-type source with small amounts of mantle input. Some of the Cana samples are highly fractionated I-type granites and affected by hydrothermal alteration.

Deoca granitoids most probably originated by partial melting of heterogeneous metagreywacke-type sources with additional contribution of mantle components. Small to large negative Eu/Eu* anomalies and depletion in MREE relative to HREE indicate that plagioclase and amphibole were major fractionating phases during magma segregation.

The major and trace element compositions of the Dalat zone granitoids indicate that they are subduction-related products. This conclusion is in good agreement with the general model of Taylor and Hayes (1983), which assumed that, from the mid-Jurassic through to mid-Cretaceous the southeast Asian margin was an Andean-type volcanic arc. Northwest subduction of the Pacific Ocean crust beneath the Eurasian continent is evidenced by widespread rhyolitic volcanism and granitic intrusions along southeast China and southeast Vietnam.

Acknowledgements

Sincere thanks are due to the DAAD for the scholarship to Thuy Nguyen T.B. We are deeply grateful to B. Hansen and an anonymous reviewer for the valuable comments and suggestions on the manuscript. We thank G. Bartholomä, M. Schumann, E. Reitter and G. Stoschek for XRF and isotopic analyses and J. Mällich for preparation of thin sections. The help of Nguyen Thu Giao and Vu Nhu Hung for guiding Thuy Nguyen T.B in the field and for discussion is greatly appreciated.

References

Altherr, R., Holl, A., Hegner, E., Langer, C., Kreuzer, H., 2000. High-potassium, calc-alkaline I-type plutonism in the European Variscides: northern Vosges (France) and northern Schwarzwald (Germany). Lithos 50, 51–73.

Bacon, C.R., Druitt, T.H., 1988. Compositional evolution of the zoned calc-alkaline magma chamber of mount Mazama, crater Lake, Oregon. Contribution to Mineralogy and Petrology 98, 224–256.

Barker, F., Farmer, G.L., Ayuso, R.A., Plafker, G., Lull, J.S., 1992. The 50 Ma granodiorites of the eastern Gulf of Alaska: melting in an accretionary prism in the forearc. Journal of Geophysic Research 97, 6757–6778.

Barr, S.M., MacDonald, A.S., 1981. Geochemistry and geochronology of late Cenozoic basalts of southeast Asia. Bulletin of the American Geologial Society. (part II) 92, 1069–1142.

Borg, L.E., Clynne, M.A., 1998. The petrogenesis of felsic calc-alkaline magmas from the southernmost Cascades, California: origin by partial melting of basaltic lower crust. Journal of Petrology 39, 1197–1222.

Bullen, T.D., Clynne, M.A., 1990. Trace element and isotopic constraints on magmatic evolution at Lassen volcanic center. Journal of Geophysic Research 95, 19671–19691.

Carter, A., Roques, A., Bristow, Kinny, P., 2001. Understanding Mesozoic accretion in southeast Asia: significance of Triassic thermotectonism (Indosinian orogeny) in Vietnam. Geology 29 (3), 211–214.

Chappell, B.W., 1999. Aluminum saturation in I-and S-type granites and the characterization of fractionated hapogranites. Lithos 46, 531–551.

Chappell, B.W., White, A.J.R., 1974. Two contrasting granite types. Pacific Geology 8, 173–174.

Chappell, B.W., White, A.J.R., 1992. I- and S-type granites in the Lachlan Fold Belt. Transactions of the Royal Society of Edinburg. Earth Sciences 83, 1–26.

Clayton, R.N., Mayeda, T.K., 1963. The use of bromine pentafluoride in the extraction of oxygen from oxides and silicates for isotopeic analysis. Geochimica et Cosmochimica Act 27, 43–52.

Dostal, J., Baragar, W.R.A., Dupuy, C., 1986. Petrogenesis of the Natkusiak continental basalts, Victoria Island, NWT. Journal of the Canadian Earth Sciences 23, 622–632.

Dostal, J., Dupuy, C., Caby, R., 1994. Geochemistry of the Neoproterozoic Tilemsi belt of Iforas (Mali, Sahara): a crustal section of an oceanic island arc. Precambrian Research 65, 55–59.

Floyd, P.A., Winchester, J.A., 1975. Magma type and tectonic setting discrimination using immobile elements. Earth and Planetary Science Letters 27, 211–218.

Förster, H.J., Tischendorf, G., Trumbull, R.B., 1997. An evaluation of the Rb vs. (Y + Nb) discrimination diagram to infer tectonic setting of silicic igneous rocks. Lithos 40, 261–293.

Grove, T.L., Donnelly-Nolan, J.M., 1986. The evolution of young silicic lavas at Medicine lake Volcano, California: implications for the origin of compositional gaps in calc-alkaline series lavas. Contribution to Mineralogy and Petrology 92, 281–302.

Guffanti, M., Clynne, M.A., Muffler, L.J.P., 1996. Thermal and mass implications of magmatic evolution in the Lassen volcanic region, California, and constraints on basalt influx to the lower crust. Journal of Geophysic Research 101, 3001–3013.

Hai, T.Q., 1986. Precambrian stratigraphy in Indochina: geology of Kampuchea, Laos and Vietnam, Scientific Publishing House, Hanoi, pp. 20–30 (in Vietnamese with English abstract).

Harmon, R.S., Gerbe, M.C., 1992. The 1982–83 eruption of Galungung volcano Java (Indonesia): Oxygen isotope geochemistry of a chemically zoned magma chamber. Journal of Petrology 33, 585–609.

Harris, N.B.W., Pearce, J.A., Tindle, A.G., 1986. Geochemical characteristics of collision-zone magmatism. In: Coward, M.P., Ries, A.C. (Eds.), Collision Tectonics, Geological Society of London, Special Publication, pp. 67–81.

Hart, S.D., Reid, M.R., 1991. Rb/Cs fractionation: A link between granulite metamorphism and the S-process. Geochimica et Cosmochimica Acta 55, 2379–2383.

Hegner, E., Roddick, J.C., Fortier, S.M., Hulbert, L., 1995. Nd, Sr, Pb, Ar and O isotopic systematics of Sturgeon lake kimberlite, Saskatchewan, Canada: Constraints on emplacement age, alteration, and source composition. Contribution to Mineralogy and Petrology 120, 212–222.

Hoskin, P.W.O., Kinny, P.D., Wyborn, D., Chappell, B.W., 2000. Identifying accessory mineral saturation during differentiation in granitoid magmas: An integrated approach. Journal of Petrology 41, 1365–1395.

Hung, V.N., 1999. Tin potential of high-aluminium granites (Datanky and Ankroet plutons) from the Dalat zone. Unpublication Master Thesis, National University of Ho Chi Minh (in Vietnamese).

Jahn, B.M., Zhou, X.H., Li, J.L., 1990. Formation and tectonic evolution of southeastern China and Taiwan: isotopic and geochemical constraints. Tectonophysics 183, 145–160.

Jonasson, K., 1994. Rhyolite volcanism in the Krafla central volcano, north-east Iceland. Bulletin of Volcanology 56, 516–528.

Khoan, P., Que, B.C., 1984. Research on the deep geological structures of Kontum area. Journal of Geology and Minerals, Hanoi 2, 174–187.

Le Maitre, R.W., 1989. A Classification of Igneous Rocks and Glossary of Terms, Blackwell, Oxford, pp. 193.

Longerich, H.P., Jenner, G.A., Jackson, S.E., Fryer, B.J., 1990. ICP-MS- a powerful new tool for high precision trace element analysis in earth sciences: evidence from analysis of selected USGS standards. Chemical Geology 83, 133–148.

Maniar, P.D., Piccoli, P.M., 1989. Tectonic discrimination of granitoids. Bulletin of the American Geological Society 101, 635–643.

Metcalfe, I., 1988. Origin and assembly of Southeast Asian continental terranes. In: Audley-Charles, M.G., Hallam, A. (Eds.), Gondwana and Tethys, 37. Geological Society of London, Special Publication, pp. 101–118.

Metcalfe, I., 1996. Pre-Cretaceous evolution of SE Asian terranes. Geological Society of London, Special Publication 106, 97–122.

Nagy, E.A., Maluski, H., Lepurier, C., Schärer, U., Thi, P.T., Leyreloup, A., Thich, U.U., 2001. Geodynamic significance of the Kontum massif in central Vietnam: composite 40Ar/39Ar ages from Paleozoic to Triassic. Journal of Geology 109, 755–770.

Nam, T.N., Yuji, S., Kentaro, T., Mitsuhiro, T., Quynh, P.V., Dung, L.T., 2001. First SHRIMP U–Pb dating of granulites from the Kontum massif (Vietnam) and tectonothermal implications. Journal of Asian Earth Sciences 19, 77–84.

O'Neil, J.R., Chappell, B.W., 1977. Oxygen and hydrogen isotope relation in the Berridale batholith, Geological Society of London, Special Publication 133, pp. 559–571.

Patĩno Douce, A.E., 1996. Effects of pressure and H_2O contents on the composition of primary crustal melts. Transactions of the Royal Society of Edinburgh. Earth Sciences 87, 11–21.

Patĩno Douce, A.E., 1999. What do experiments tell us about the relative contributions of crust and mantle to the origin of granitic magmas? . In: Castro, A., Fernandez, C., Vigneressese, J.L. (Eds.), Understanding Granites: Intergrating New and Classical Techniques, 168. Geological Society of London, Special Publication 168, pp. 55–75.

Pearce, J.A., Harris, N.B., Tindle, A.G., 1984. Trace element discrimination diagrams for the tectonic interpretation of granitic rocks. Journal of Petrology 25, 956–983.

Roberts, M.P., Clemens, J.D., 1993. Origin of high-potassium, calc-alkaline, I-type granitoids. Geology 21, 825–828.

Rogers, G., Hawkesworth, C.J., 1989. A geochemical traverse across the North Chilean Andes: evidence for crust generation from the mantle wedge. Earth and Planetary Science Letters 91, 271–285.

Romick, J.D., Kay, S.M., Kay, R.W., 1992. The influence of amphibole fractionation on the evolution of calc-alkaline andesite and dacite tephra from the central Aleutians, Alaska. Contribution to Mineralogy and Petrology 112, 101–118.

Sajona, F.G., Maury, R.C., Bellon, H., Cotton, J., Defant, M., 1996. High field strength elements of Pliocene-Pleistocene island-arc basalts Zamboanga Peninsula, Western Mindanao (Philippines). Journal of Petrology 37, 693–726.

Searle, M.P., Fryer, B.J., 1986. Garnet- tourmaline- and muscovite-bearing leucogranites, gneisses and migmatites of the higher Himalayas from Zanska, Kulu, Lahoul and Kashmir. In: Coward, M.P., Ries, A.C. (Eds.), Collision Tectonics, Geological Society of London, Special Publication 19, pp. 185–202.

Sengör, A.M.C., Altiuner, D., Cin, A., Ustaömer, T., Hsü, K.J., 1988. Origin and assembly of the Tethyan orogenic collage at the expense of Gondwana land. Gondwana and Tethys, Geological Society of London, Special Publication 37, pp. 119–181.

Shand, S.J., 1927. Eruptive Rocks, D. Van Nostrand Company, New York, pp. 360.

Sun, S.S., 1982. Chemical composition and origin of the Earth's primitive mantle. Geochimica et Cosmochimica Acta 46, 179–192.

Taylor, H.P., 1968. Oxygen isotope geochemistry of igneous rocks. Contribution to Mineralogy and Petrology 19, 1–71.

Taylor, H.P., 1978. Oxygen and hydrogen isotope studies of plutonic granitic rocks. Earth and Planetary Science Letters 38, 177–210.

Taylor, B., Hayes, D.E., 1983. Origin and history of the South China Sea Basin. The tectonic and geologic evolution of Southeast Asian seas and islands, part 2. In: Hayes, D.E., (Ed.), Geophysical Monograph 27. American Geophysic Union, Washington, pp. 23–56.

Taylor, S.R., Mclennan, S.M., 1985. The Continental Crust: Its Composition and Evolution, Blackwell, Oxford, pp. 312.

Tepper, J.H., Nelson, B.K., Bergantz, G.W., Irving, A.J., 1993. Petrology of the Chilliwack batholith, North Cascades, Washington: generation of calc-alkaline granitoids by melting of mafic lower crust with variable water fugacity. Contribution to Mineralogy and Petrology 113, 333–351.

Thang, D.N., Duyen, D.T., 1988. Geological map of Dongnai-Benkhe region with the scale 1:200,000. Department of Geology and Minerals, Hanoi (in Vietnamese).

Thi, P.T., 1985. Metamophic complexes of the Socialist Republic of Vietnam. In: Man, L.S., (Ed.), Explanatory Text of the Metamorphic Map of South and East Asia (1:1000000), CGMW-UNESCO, pp. 90–95.

Thompson, A.B., 1996. Fertility of crustal rocks during anatexis. Transactions of the Royal Society of Edinburgh. Earth Sciences 87, 1–10.

Thuy Nguyen, T.B., Satir, M., Siebel, W., Chen, F., 2000. Geochronology of granitoids from the Dalat zone, southern Vietnam. European Journal of Mineralogy, Abstract, 12–1, 139.

Thuy Nguyen, T.B., Satir, M., Siebel, W., Chen, F., 2002. Granitoids in the Dalat zone, southern Vietnam: age constraints on magmatism and regional geological implications. International Journal of Earth Sciences (submitted).

Tien, P.C., An, L.D., Bach, L.D., 1991. Geology of Cambodia, Laos and Vietnam (geological map 1: 1, 000, 000) and its explanatory note. Geological Survey of Vietnam 158 pp.

Trung, H., Bao, X.N., 1980. The classification of intrusive magma formations, southern Vietnam. Journal of Geology, Hanoi 40, 39–56 (in Vietnamese).

Vielzeuf, D., Holloway, J.R., 1988. Experimental determination of fluid-absent melting relations in the pelitic relation in pelitic system. Contribution to Mineralogy and Petrology 98, 357–376.

Weaver, B.L., 1990. Geochemistry of highly-undersaturated ocean island basalt suites from the South Atlantic Ocean: Fernando de Noronha and Trindade islands. Contribution to Mineralogy and Petrology 105, 502–515.

Whalen, J.B., Currie, K.L., Chappell, B.W., 1987. A-type granites: Geochemical characteristics and discrimination. Contribution to Mineralogy and Petrology 95, 420–436.

White, A.J.R., Chappell, B.W., 1983. Granitoid types and their distribution in the Lachlan Fold Belt, southeastern Australia. Geological Society of America Memoir 159, 21–34.

Wolf, M.B., Wyllie, J.P., 1994. Dehydration melting of amphibolite at 10 kbar: The effects of temperature and time. Contribution to Mineralogy and Petrology 115, 369–383.

Woodhead, S.D., Harmon, S.R., Fraser, D.G., 1987. O, S, Sr and Pb isotope variations in volcanic rocks from Northern Mariana Islands: Implications for crustal recycling in intraoceanic areas. Earth Planetary Science Letters 83, 39–52.

Wyllie, P.J., 1984. Constraints imposed by experimental petrology on possible and impossible magma sources and products. Transactions of the Royal Society of London A310, 439–456.